2018 Spring Technical Meeting
Central States Section of the Combustion Institute
May 20–22, 2018
Minneapolis, Minnesota

Auto-ignitive deflagration of CH_4 blended DME/Air mixtures with composition stratification

Swapnil Desai[1*], *Ramanan Sankaran*[1,2], *and Hong G. Im*[3]

[1]*Bredesen Center for Interdisciplinary Research and Graduate Education, University of Tennessee, Knoxville, TN 37996-3394, USA*
[2]*Oak Ridge National Laboratory, Oak Ridge, TN 37831-6008, USA*
[3]*Clean Combustion Research Center, King Abdullah University of Science and Technology, Thuwal 23955-6900, Saudi Arabia*
[*]*Corresponding author:* sdesai9@vols.utk.edu

Abstract: Front propagation speeds from one dimensional simulations of DME/Air and DME/CH_4/Air mixtures under engine relevant conditions are presented with reduced kinetics and transport. Different time scales of monochromatic inhomogeneities in DME concentration and varying DME-CH_4 blending ratios are explored to understand its subsequent effect on the propagation speed as well as the ensuing transition from deflagration to spontaneous propagation. It is found that for a given time-scale, the instantaneous peak propagation speed achieved by a front as well as its overall variation is significantly affected by the level of CH_4 concentration in the mixture. Specifically, at relatively smaller time scales, the magnitude of variation in the instantaneous propagation speed is found to subside as the level of CH_4 concentration in the mixture is increased. An opposite trend is observed at comparatively larger time scales, wherein, a rapid change in the instantaneous propagation speed is observed with an increase in the level of CH_4 concentration. This study provides evidence as to how the propagation speed of a single fuel flame varies compared to a dual fuel flame under the influence of composition stratification.
Keywords: ***Flame Speed, Flame Dynamics, Spontaneous Propagation, Deflagration, RCCI***

1. Introduction

Over the last decade, various experimental and numerical studies have demonstrated that advanced strategies of internal combustion (IC) engines such as homogeneous charge compression ignition (HCCI) and reactivity controlled compression ignition (RCCI) often involve mixed modes of combustion due to the presense of a highly reactive premixed charge [1–9]. In such cases, flames and auto-ignition processes are simultaneously contributing to the overall process of combustion and subsequent heat release. The presence of such multiple combustion modes presents challenges in controlling the pressure rise rate and ignition timing, particularly under high load conditions. Nonetheless, compared to single fuel premixed compression ignition strategies, dual fuel strategies exhibit a better controllability of the combustion process without sacrificing high thermal efficiency, improved fuel consumption and ultra low pollutant emissions [10, 11]. RCCI uses in-cylinder fuel blending with at least two fuels of different reactivity and multiple injections to control in-cylinder fuel reactivity to optimize combustion phasing, duration and magnitude. The process involves introduction of a low reactivity fuel into the cylinder to create a well-mixed charge

of low reactivity fuel, air and recirculated exhaust gases. The high reactivity fuel is injected before ignition of the premixed fuel occurs using single or multiple injections directly into the combustion chamber [11, 12]. Under actual operating conditions, the originating fronts in such engines may have fundamentally different behavior at widely different speeds depending on the mixture conditions. The propagation speed of these fronts directly affects the thermal efficiency. A lower flame speed increases the combustion duration and weakens the constant-volume combustion process, and thus reduces the thermal efficiency. On the other hand, a very high flame speed indicates a rapid combustion reaction rate, which increases the constant-volume combustion process but is also the main challenge in extending the operating loads of such engines. Therefore, an accurate prediction of front propagation speeds at engine relevant conditions is of fundamental importance to better understand RCCI and similar mixed modes of combustion.

Traditionally, the deflagrative flame speed is evaluated as an eigen value for a planar front in an infinite domain [13], wherein the mixture is presumed to be non-reactive at far upstream, with essentially an infinite ignition delay time τ compared to the characteristic flame time τ_f, until thermal diffusion from the propagating front makes it reactive via temperature rise and radical diffusion. The freely propagating laminar flame speed of a sufficiently cold reactant mixture is therefore, independent of the domain size or the flame location. However, at auto-ignitive conditions, which exist for many combustion devices including IC engines, the front speed is no longer independent of the flame position or boundary conditions. This is because flammable mixtures have a finite τ and therefore the reactant mixture is changing ahead of the flame. As a result, in principle, a steady-state solution does not exist. This sensitivity of the laminar flame solutions to the domain size has also been observed in previous numerical studies [14] but not adequately discussed. More recently, Krisman et al. [15] explored the sensitivity of the flame location and the characteristic flame time to the inlet velocity for fuels exhibiting single and two stage ignition in order to estimate a reference laminar flame speed at autoignitive conditions. It was found that single (two) stage ignition fuel exhibit one (two) peak(s) in the flame location sensitivity. The study also showed that the transition from flame propagation to spontaneous autoignition front occurs very gradually over a wide range of inlet velocities. Based on the results of the study, it was estimated that the laminar flame speed at autoignitive conditions is $\approx$ 1 - 2 m/s for fuels exhibiting either single or two stage ignition.

Earlier experimental [16, 17] and simulation ([5, 18, 19] and references therein) works have demonstrated that preheated, fuel lean mixtures characteristic of HCCI and RCCI engines are capable of supporting reaction fronts propagating at subsonic speeds ranging from 0.5 m/s to 160 m/s, without any high frequency oscillations in the cylinder pressure. This wide range of propagation speeds suggests that the fronts arising under such conditions have controlling mechanisms that may be distinct from typical deflagration fronts. Zeldovich [20] first identified the regimes of a reaction front propagating through a non-uniform reactive mixture. Of particular relevance to modern IC engines utilizing mixed modes of combustion are: (i) spontaneous propagation, where propagation is driven by the sequential auto-ignition of the mixture and (ii) premixed deflagration, in which conduction and diffusion play a major role in propagation. Subsequently, a number of studies attempted to provide a practical and meticulous way to identify the front regimes. A criterion based on the ratio of characteristic temperature gradients was suggested by Gu et al. [21]. Sankaran et al [22] identified the regimes based on the ratio of deflagration speed to the ignition delay gradients. Another criterion based on the Damköhler number along the front norm has been suggested by Bansal and Im [4]. Use of computational singular perturbation to automate the char-

Nomenclature

λ_1	Position of the cool flame from the inlet (mm)	$\triangle x$	Uniform grid resolution (μm)
λ_2	Position of the main/hot flame from the inlet (mm)	A	Amplitude of fluctuation in DME composition
ϕ_b	Overall equivalence ratio at the flame base	c	Blending ratio
ϕ_{DME}	Equivalence ratio with respect to DME	L	Domain length (mm)
ϕ_{O_2}	Equivalence ratio with respect to CH_4	S	Steady global consumption speed (m/s)
$\phi_{overall}$	Overall equivalence ratio	S_c	Unsteady global consumption speed (m/s)
τ_0	Time scale of fluctuation in DME concentration (μs)	T_b	Temperature at the flame base (K)
τ_1	1^{st} stage auto-ignition delay time (ms)	Y_{CH_4}	Mass fraction of CH_4
τ_2	2^{nd} stage auto-ignition delay time (ms)	Y_{DME}	Mass fraction of DME
		Y_{O_2}	Mass fraction of O_2

acterization of the nature of the fronts have also been attempted [23]. Identifying the effects of these two regimes as well as the transition between the two on the originating front propagation is of fundamental interest for high-fidelity modeling of modern IC engines utilizing mixed-mode combustion.

While there has been a significant amount of studies on the transition from ignition to premixed deflagration [24] as well as from premixed deflagration to end-gas auto-ignition and detonation [21, 25, 26], few studies are found on the transition from premixed deflagration to spontaneous propagation and its subsequent effect on the propagation speed of the emerging fronts. Deng et al. [27, 28] investigated the structure and dynamics of laminar nonpremixed dimethyl ether (DME)/Air coflow flames at elevated temperatures and pressures under the influence of oscillating inlet velocities. It was found that in an oscillating reacting flow, transition between a multibrachial autoignition front and a tribrachial flame occurs periodically. However, unlike the harmonic velocity oscillation, the combustion mode transition was observed to hysteretic. It was further shown that the finite induction time for autoignition resulted in the hysteretic behavior. Although a cyclic transition from tribrachial deflagration to multibrachial auto-ignition was demonstrated in these studies, the chosen oscillation frequencies were relatively low and the resulting time scales didn't necessarily correspond to τ, the ignition delay time of the fuel/air mixture. Besides, these experimental and computational investigations mainly focused on single fuel blends and did not investigate the effect of reactivity stratification, the strategy used in RCCI engines for controlling the pressure rise rate and ignition timing, on the transition of combustion modes of the originating fronts.

Based on the above discussion, the objective of the present study is : 1) to provide a parametric mapping of unsteady deflagration speed of an auto-ignitive methane (CH_4) blended DME/Air mixture which has contributions from multiple combustion modes under monochromatic DME concentration stratification at different time-scales and 2) to compare the relative difference in the propagation speed of a single fuel flame with respect to a dual fuel flame with varying DME-CH_4 blending ratio. Since the low reactivity fuel (i.e. CH_4) is typically premixed and the high reactivity fuel (i.e. DME) is direct-injected in RCCI engines, CH_4 distribution is nearly uniform throughout the combustion chamber. The direct-injected DME would then impose a distribution of the overall equivalence ratio i.e. ϕ_{overall}, defined in section 2, onto the uniform CH_4 distribution which has been demonstrated in [5]. The start-of-injection timing is tweaked [8] as per requirements for controlling the stratification of direct-injected, high reactivity fuel (i.e. DME) in RCCI engines. The temporal variation in either single or multiple direct injections of the high reactivity fuel (i.e. DME) would then translate into pockets of stratified composition field in the combustion chamber. To simulate this, monochromatic temporal fluctuations in DME concentration are imposed on a dual fuel flame such that it propagates into a stratified DME concentration field of a given size. The dual fuel blend of DME-CH_4 is chosen for the present study since DME is one of the simplest fuel molecules that exhibits two-stage ignition, a characteristic exhibited by many practical hydrocarbon fuels and CH_4, the main component of natural gas has been shown to aid in extending the high load limit of RCCI combustion due to its resistance-to-autoignition quality [29]. One-dimensional parametric simulations are conducted and the results are systematically analyzed. It must be noted that, depending upon the level of preheating and the type of high reactivity fuel used, the originating fronts in RCCI engines may exhibit either a single (without low temperature chemistry) or a dual staged (with low temperature chemistry) thermal structure. However, the present study focuses only on the behavior of dual staged flame under the influence of imposed stratification.

2. Numerical procedure and initial conditions

Fully resolved numerical simulations are performed using KARFS (KAUST Adaptive Reacting Flow Solver) [30] that solves the compressible Navier-Stokes, continuity, species and energy equations. Spatial derivatives are approximated with an eighth-order finite difference operator [31] along with a tenth-order explicit filter, and solution is advanced in time with a six-stage fourth-order Runge-Kutta method [32]. A reduced DME chemical mechanism [33] consisting of 30 species and 175 reactions with 9 species identified as global quasi-steady state species is used in the present study. The employed mechanism has been systematically reduced and validated from a detailed mechanism [34]. Previous studies [35–37] have demonstrated that the detailed mechanism is able to accurately reproduce the flame speeds and ignition delay times of DME–Air, CH_4–Air as well as DME-CH_4-Air mixtures for a wide range of operating conditions. For all the cases being studied here, the difference in magnitude of steady propagation speed, S and the two ignition delay times, τ_1 and τ_2, using either of the two mechanisms is found to be less than 4%.

To understand the effect of varying DME-CH_4 blending ratio, c in conjunction with a change in the frequency/time-scale of reactivity stratification on S, one dimensional simulations are conducted for three canonical cases: DME100, DME75 and DME62.5 with identical mean unburnt mixture temperature T_0=800 K and mean pressure P_0=40 atm. To avoid large pressure waves within the domain, non-reflective boundary conditions are imposed at the inlet and the outlet as

described in [38]. Due to open boundaries, the thermodynamic pressure remains constant, thereby allowing a statistically stationary limit cycle behaviour to be produced for the unsteady cases. Here, the blending ratio c is defined as the mass fraction of CH_4 in the binary fuel blend, ranging from 0 (pure DME) to 1.0 (pure CH_4). The various physical and numerical parameters used in the three cases are listed in Table 1. In each case, the uniform grid resolution, $\triangle$x, corresponds to a minimum of 12 grid points across the thinnest radical and reaction rate layers in the combustion front. The grid convergence test is fully performed to ensure the numerical accuracy of the solutions.

Case	τ_1 (ms)	τ_2 (ms)	S (m/s)	L (mm)	c	$\triangle x$ (μm)	ϕ_{DME}	ϕ_{CH_4}	ϕ_{overall}
DME100	0.37	1.18	2	8	0	3.4	0.4	0	0.4
DME75	0.39	2.13	2	10	0.25	5.3	0.3	0.1	0.4
DME62.5	0.41	3.34	2	20	0.375	7	0.25	0.15	0.4

Table 1: Physical and numerical parameters corresponding to the three cases

For each case, a series of steady solutions are computed by varying the high temperature flame position i.e. λ_2, for which the correct inflow velocity is determined as an eigenvalue in Cantera [39] to satisfy a given steady solution. In the unsteady calculations, a selected steady solution is used initially at a fixed inflow velocity while the inflow DME concentration is varied in time as:

$$\mathrm{Y_{DME}(t) = Y_{DME}(t) + A\sin(\frac{2\pi t}{\tau_0})} \tag{1}$$

and at all times the deficit or excess of DME concentration is compensated by adjusting the air concentration. In eq. 1, A is the amplitude of stratification in DME concentration, t is time and τ_0 is the time scale of stratification. Since, dual fuel blends constitute unique challenges in terms of defining mixture parameters such as mixture fraction or equivalence ratio, three types of equivalence ratio are defined as per the previous approaches [8, 33] for clarity. The equivalence ratio with respect to DME and CH_4 are computed as:

$$\phi_{\text{DME}} = \nu_{\text{DME}} \frac{\mathrm{Y_{DME,u}}}{\mathrm{Y_{O_2,u}}} \tag{2}$$

and

$$\phi_{\text{CH}_4} = \nu_{\text{CH}_4} \frac{\mathrm{Y_{CH_4,u}}}{\mathrm{Y_{O_2,u}}} \tag{3}$$

where ν_{DME} and ν_{CH_4} are the stoichiometric oxygen-to-fuel mass ratios for a particular fuel [40]. Equations 2 and 3 assume that all of the local oxygen is available to react with both fuels, which is not the case in real operating conditions. Therefore, they do not necessarily represent equivalence ratios in a strict sense, but instead indicate normalized concentrations of DME and CH_4 respectively. Additionally, an overall equivalence ratio, ϕ_{overall} is computed at every grid point based on the combined local fuel (DME+CH_4) and oxygen concentrations. This is identical to the equivalence ratio definition that is typically used in single fuel systems. Since earlier studies [5] demonstrated that a larger concentration of the high reactivity fuel provides a greater degree of flame propagation, ϕ_{DME} is purposefully kept higher than ϕ_{CH_4} in cases DME75 and DME62.5 respectively. This further supports the assumption that a dual fuel deflagration front has already

been established in the domain. For each case, calculations are carried out with DME concentration stratification at six different timescales i.e. $\tau_0 = \tau_1/2, \tau_1, 2\tau_1, \tau_2/2, \tau_2, 2\tau_2$. For the time scales corresponding to τ_1 i.e. $\tau_0 = \tau_1/2, \tau_1$ and $2\tau_1$, the amplitude of stratification in DME concentration, $A = 0.06$ while for those corresponding to τ_2 i.e. $\tau_0 = \tau_2/2, \tau_2$ and $2\tau_2$, $A = 0.02$. The magnitude of A for the respective time scales was chosen so as to ensure numerical stability and avoid flame blow-off. The resulting root-mean-square fluctuation in A, nevertheless, is of the same order as has been previously used [4, 5]. It must be noted that the purpose of the present investigation is to determine the difference in propagation speeds of a single fuel flame and dual fuel flame under composition stratification and not to reproduce the exact conditions from a specific set of engine experiments.

3. The steady flame behavior

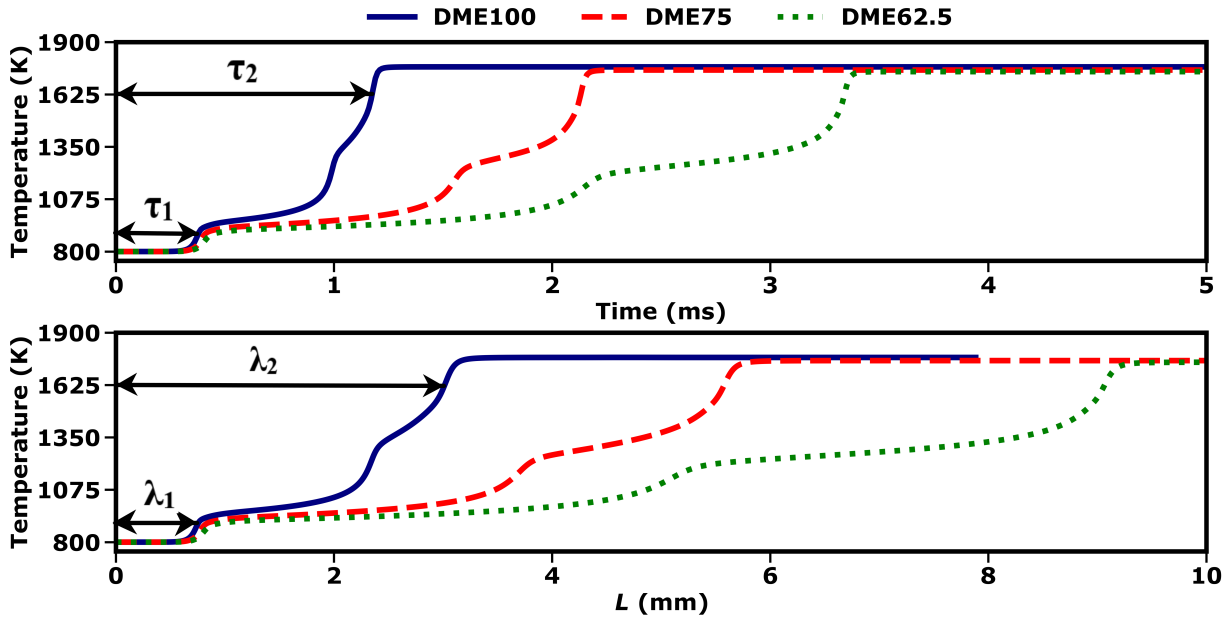

Figure 1: Initial temporal and spatial profiles of temperature for the three cases

The two homogeneous auto-ignition delay times, τ_1 and τ_2, corresponding to the 1st and 2nd stage ignition have been measured at the points of maximum heat release for that respective stage as shown in Fig 1. Likewise, the spatial location where the low temperature cool flame and the high temperature flame get anchored in the domain are denoted by λ_1 and λ_2 respectively. Analogous to the measurement of τ_1 and τ_2, λ_1 and λ_2 have also been measured at the points maximum heat release for that respective stage. The overall temperature rise in each case is around 950 K. Detailed studies [15, 41] have been carried out for the steady state analysis of front propagation speed at auto-ignitive conditions with respect to a variation in inlet temperature and inlet flow velocity respectively. Hence, for brevity, the steady state analysis in the present study is carried out mainly for validating the selection of initial conditions as correctly representing deflagration regime and comparing the expected rise in S with respect to high temperature flame location, λ_2, for the three cases. Fig. 2 shows the variation in steady consumption speed S with respect to a

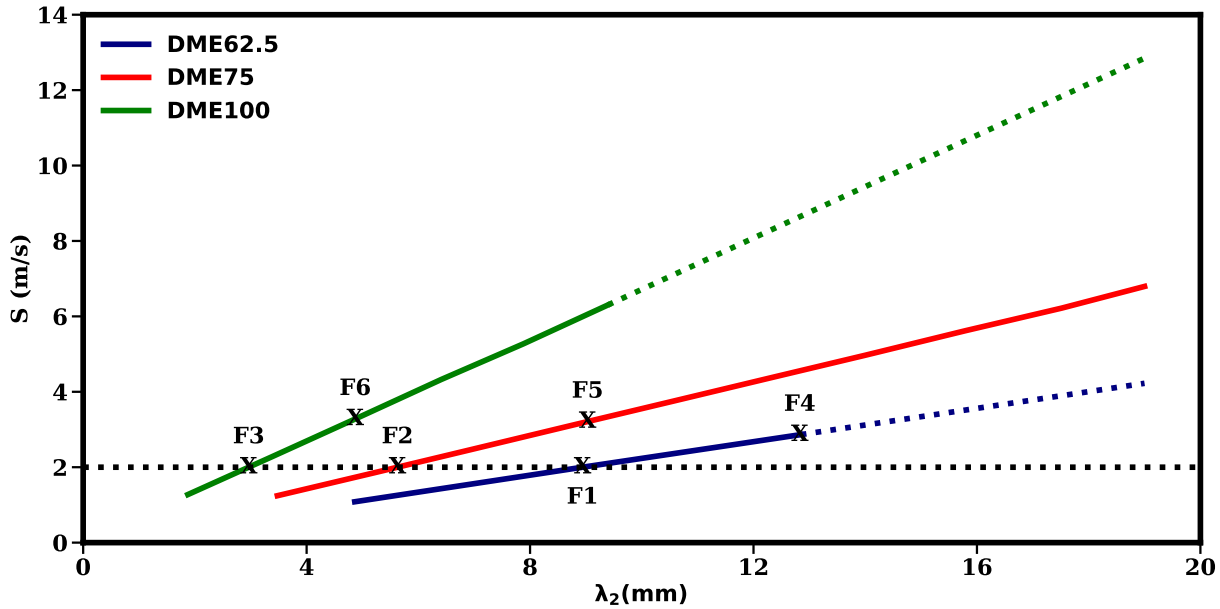

Figure 2: Variation in S with λ_2 for the three cases

change in the position of the high temperature flame, λ_2. Here, S represents the steady global consumption speed and has been defined based on the mass balance of a stationary flame from the perspective of oxygen consumption [40]

$$S = -\frac{1}{\rho_u Y^u_{O_2}} \int \dot{\omega}_{O_2} dx \tag{4}$$

where $Y^u_{O_2}$ is the mass fraction of O_2 in the unburnt gas, ρ_u is the unburnt gas density and $\dot{\omega}_{O_2}$ is the oxygen consumption rate. For all the cases, S is observed to rise with an increase in λ_2. However, for case DME100, S rises at the fastest rate while for case DME62.5, the rise in S is the slowest. This is because τ_2 in case DME100 is the smallest. As a result, the overall induction time required for the mixture to auto-ignite and enter the spontaneous propagation regime is the lowest in case DME100. The fronts at points F1, F2 and F3 depicted in Fig. 2 represent the initial condition of the respective cases that has been used for the unsteady calculations. Note that S = 2 m/s at all the fronts F1, F2 and F3 which is of the same order as that of the reference laminar flame speed at auto-ignitive conditions estimated in [15]. Therefore, the combustion front at each of the points F1, F2 and F3 can be considered to be in the deflagration regime with negligible thermal runaway of the upstream mixture. As the flame is moved downstream at points F4, F5 and F6 respectively, the reactivity of the upstream mixture increases before it enters the flame, thereby actuating a linear increase in S and a subsequent transition in the combustion mode.

4. Response to unsteady DME concentration fluctuations

In this section, the dual fuel flame response to the imposed stratification in DME concentration is presented. Since, the flame response to the very near upstream conditions is of more practical importance, the unsteady results have been presented with respect to the flame base rather than

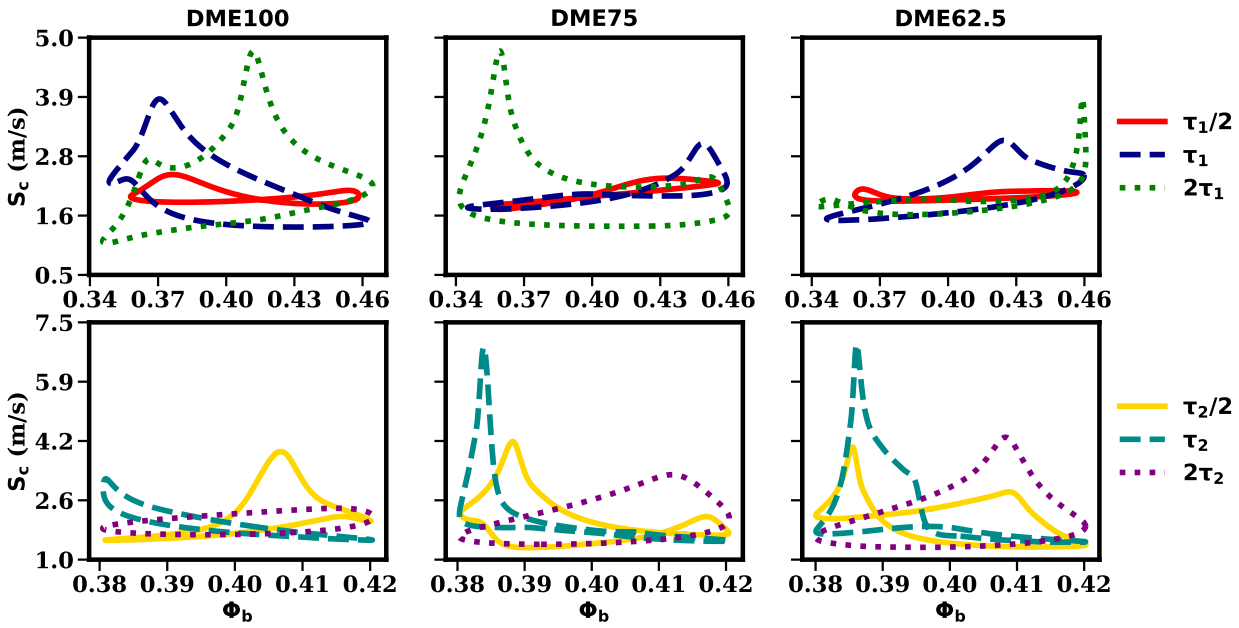

Figure 3: Variation in S_c with ϕ_b for different τ_0

the inlet. Here, the flame base has been defined as the spatial location where T = 820 K. In Fig. 3, S_c represents the unsteady global consumption speed and has been defined with respect to O_2, identical to S, as shown in eq. 1. ϕ_b represents the overall equivalence ratio at the flame base. For each case, the top row in Fig. 3 shows the flame response at the three time scales corresponding to τ_1 while the bottom row depicts the flame response at the three time scales corresponding to τ_2. It is clearly seen that the variation in S_c with respect to ϕ_b is not harmonic but is rather hysteretic as has also been previously observed in [28, 44]. Except for the largest time scale i.e. $\tau_0 = 2\tau_2$ in each case, the limit cycle, exhibits a complex shape with either single or dual peaks depending upon the imposed value of τ_0 and the blending ratio, c. At all time scales of imposed stratification, the flame response in case DME100 is observed to be strikingly different than that in case DME75. Further increase in CH_4 concentration is not found to substantially affect the flame response as observed from the flame behavior in case DME62.5. For the same variation in ϕ_b, when $\tau_0 \leq 2\tau_1$, the instantaneous peak S_c and its overall variation gradually subsides with an increase in CH_4 concentration. At relatively shorter time scales, the imposed variation in Y_{DME} is substantially attenuated due to diffusive effects within the upstream zone and the induction time available for the unburnt mixture to auto-ignite is considerably shorter. Also, due to a higher concentration of CH_4, τ_2 in case DME62.5 is about 3 times higher than that in case DME100 which makes the mixture in case DME62.5 more resistant to autoignition. As a result, the high temperature flame remains mostly unaffected by the imposed stratification in case DME62.5. An opposite trend in the flame response is observed for time scales corresponding to τ_2, specifically when $\tau_2/2 < \tau_0 < 2\tau_2$. For an identical variation in ϕ_b, when $\tau_2/2 < \tau_0 < 2\tau_2$, there is a substantial rise in the magnitude of instantaneous peak S_c with an increase in CH_4 concentration. This shows that although the mixture in case DME62.5 is more resistant-to-autoignition, the relatively larger time scales provide sufficient induction time for the upstream mixture to become highly reactive and when $\tau_0 = \tau_2$, the mixture auto-ignites leading to a sharp increase in instantaneous S_c. Hence, it can be concluded

that under the effect of composition stratification, a single fuel flame behaves notably distinct than a dual fuel flame. Future work involves carrying out the displacement speed budget analysis in order to quantify the periodic transition of combustion modes.

5. Conclusion

The propagation speed of an auto-ignitive CH_4 blended DME/Air mixture subjected to different time scales of stratification in DME concentration is computationally studied in a statistically stationary, one dimensional planar configuration with reduced kinetics and transport. Additionally, three different values of blending ratio, c, are investigated to examine the subsequent effect on the front propagation speed. Based on the flame response to the imposed stratification in DME concentration, following conclusions can be drawn:
1) Irrespective of the blending ratio, c, at very small time scales i.e. $\tau_0 = \tau_1/2$, the flame response is negligible. When τ_0 is between τ_1 and τ_2, the limit cycle exhibits either a single or a dual peaks in instantaneous S_c. At very large time scales i.e. $\tau_0 = 2\tau_2$, the flame response is found to revert to an elliptical path.
2) At relatively smaller time scales, the overall variation in instantaneous S_c gradually subsides with an increase in the blending ratio, c due to diffusive effects in the upstream zone coupled with an increase in the resistance to auto-ignition characteristics of the mixture and a considerably shorter induction time. At comparatively larger time scales, due to a longer induction time available for the mixture to auto-ignite, an abrupt change in instantaneous S_c is observed when c is increased from 0 to 0.25. Further increase in c only shows a minor change in the overall flame behavior.

Acknowledgments

This work was sponsored by competitive research funding from King Abdullah University of Science and Technology. This research used resources of the Oak Ridge Leadership Computing Facility at ORNL, which is supported by the Office of Science of the U.S. Department of Energy under Contract No. DE-AC05-00OR22725.

References

[1] C. Strozzi, A. Mura, J. Sotton, and M. Bellenoue, Experimental analysis of propagation regimes during the autoignition of a fully premixed methane−air mixture in the presence of temperature inhomogeneities, Combustion and Flame 159 (2012) 3323–3341.

[2] Z. Wang, J. X. Wang, S. J. Shuai, and Q. J. Ma, Effects of Spark Ignition and Stratified Charge on Gasoline HCCI Combustion With Direct Injection, SAE Technical Paper SAE International, (2005).

[3] D. Assanis, S. W. Wagnon, and M. S. Wooldridge, An experimental study of flame and autoignition interactions of iso-octane and air mixtures, Combustion and Flame 162 (2015) 1214–1224.

[4] G. Bansal and H. G. Im, Autoignition and front propagation in low temperature combustion engine environments, Combustion and Flame 158 (2011) 2105–2112.

[5] A. Bhagatwala, R. Sankaran, S. Kokjohn, and J. H. Chen, Numerical investigation of spontaneous flame propagation under RCCI conditions, Combustion and Flame 162 (2015) 3412–3426.

[6] J. E. Dec and W. Hwang, Characterizing the Development of Thermal Stratification in an HCCI Engine Using Planar-Imaging Thermometry, SAE Int. J. Engines 2 (2009) 421–438.

[7] J. E. Dec, W. Hwang, and M. Sjöberg, An investigation of thermal stratification in HCCI engines using chemiluminescence imaging, tech. rep. Report No., SAE Technical Paper, 2006.

[8] S. Kokjohn, R. D. Reitz, D. Splitter, and M. Musculus, Investigation of fuel reactivity stratification for controlling PCI heat-release rates using high-speed chemiluminescence imaging and fuel tracer fluorescence, SAE International Journal of Engines 5 (2012) 248–269.

[9] Q. Tang, H. Liu, M. Li, M. Yao, and Z. Li, Study on ignition and flame development in gasoline partially premixed combustion using multiple optical diagnostics, Combustion and Flame 177 (2017) 98–108.

[10] S. L. Kokjohn, R. M. Hanson, D. Splitter, and R. Reitz, Fuel reactivity controlled compression ignition (RCCI): a pathway to controlled high-efficiency clean combustion, International Journal of Engine Research 12 (2011) 209–226.

[11] R. D. Reitz and G. Duraisamy, Review of high efficiency and clean reactivity controlled compression ignition (RCCI) combustion in internal combustion engines, Progress in Energy and Combustion Science 46 (2015) 12–71.

[12] A. Paykani, A.-H. Kakaee, P. Rahnama, and R. D. Reitz, Progress and recent trends in reactivity-controlled compression ignition engines, International Journal of Engine Research 17 (2016) 481–524.

[13] A. Merzhanov and B. Khaikin, Theory of combustion waves in homogeneous media, Progress in Energy and Combustion Science 14 (1988) 1–98.

[14] J. Pan, H. Wei, G. Shu, Z. Chen, and P. Zhao, The role of low temperature chemistry in combustion mode development under elevated pressures, Combustion and Flame 174 (2016) 179–193.

[15] A. Krisman, E. R. Hawkes, and J. H. Chen, The structure and propagation of laminar flames under autoignitive conditions, Combustion and Flame 188 (2018) 399–411.

[16] X. Ma, Z. Wang, C. Jiang, Y. Jiang, H. Xu, and J. Wang, An optical study of in-cylinder CH_2O and OH chemiluminescence in flame-induced reaction front propagation using high speed imaging, Fuel 134 (2014) 603–610.

[17] X. Ma, Y. Li, Y. Qi, H. Xu, S. Shuai, and J. Wang, Optical study of throttleless and EGR-controlled stoichiometric dual-fuel compression ignition combustion, Fuel 182 (2016) 272–283.

[18] J. Martz, H. Kwak, H. Im, G. Lavoie, and D. Assanis, Combustion regime of a reacting front propagating into an auto-igniting mixture, Proceedings of the Combustion Institute 33 (2011) 3001–3006.

[19] J. B. Martz, G. A. Lavoie, H. G. Im, R. J. Middleton, A. Babajimopoulos, and D. N. Assanis, The propagation of a laminar reaction front during end-gas auto-ignition, Combustion and Flame 159 (2012) 2077–2086.

[20] Y. Zeldovich, Regime classification of an exothermic reaction with nonuniform initial conditions, Combustion and Flame 39 (1980) 211–214.

[21] X. Gu, D. Emerson, and D. Bradley, Modes of reaction front propagation from hot spots, Combustion and Flame 133 (2003) 63–74.

[22] R. Sankaran, H. G. Im, E. R. Hawkes, and J. H. Chen, The effects of non-uniform temperature distribution on the ignition of a lean homogeneous hydrogen air mixture, Proceedings of the Combustion Institute 30 (2005) 875–882.

[23] S. Gupta, H. G. Im, and M. Valorani, Analysis of n-heptane auto-ignition characteristics using computational singular perturbation, Proceedings of the Combustion Institute 34 (2013) 1125–1133.

[24] W. Sun, S. H. Won, X. Gou, and Y. Ju, Multi-scale modeling of dynamics and ignition to flame transitions of high pressure stratified n-heptane/toluene mixtures, Proceedings of the Combustion Institute 35 (2015) 1049–1056.

[25] Y. Ju, W. Sun, M. P. Burke, X. Gou, and Z. Chen, Multi-timescale modeling of ignition and flame regimes of n-heptane-air mixtures near spark assisted homogeneous charge compression ignition conditions, Proceedings of the Combustion Institute 33 (2011) 1245–1251.

[26] P. Dai, C. Qi, and Z. Chen, Effects of initial temperature on autoignition and detonation development in dimethyl ether/air mixtures with temperature gradient, Proceedings of the Combustion Institute 36 (2017) 3643–3650.

[27] S. Deng, P. Zhao, M. E. Mueller, and C. K. Law, Stabilization of laminar nonpremixed DME/air coflow flames at elevated temperatures and pressures, Combustion and Flame 162 (2015) 4471–4478.

[28] S. Deng, P. Zhao, M. E. Mueller, and C. K. Law, Flame dynamics in oscillating flows under autoignitive conditions, Combustion and Flame 168 (2016) 75–82.

[29] D. E. Nieman, A. B. Dempsey, and R. D. Reitz, Heavy-duty RCCI operation using natural gas and diesel, SAE International Journal of Engines 5 (2012) 270–285.

[30] F. E. H. Perez, N. Mukhadiyev, X. Xu, A. Sow, B. J. Lee, R. Sankaran, and H. G. Im, Direct numerical simulations of reacting flows with detailed chemistry using many-core/GPU acceleration, Computers and Fluids (2017).

[31] C. A. Kennedy and M. H. Carpenter, Several new numerical methods for compressible shear-layer simulations, Applied Numerical Mathematics 14 (1994) 397–433.

[32] C. A. Kennedy, M. H. Carpenter, and R. M. Lewis, Low-storage, Explicit Runge-Kutta Schemes for the Compressible Navier-Stokes Equations, Appl. Numer. Math. 35 (2000) 177–219.

[33] A. Bhagatwala, Z. Luo, H. Shen, J. A. Sutton, T. Lu, and J. H. Chen, Numerical and experimental investigation of turbulent DME jet flames, Proceedings of the Combustion Institute 35 (2015) 1157–1166.

[34] Z. Zhao, M. Chaos, A. Kazakov, and F. L. Dryer, Thermal decomposition reaction and a comprehensive kinetic model of dimethyl ether, International Journal of Chemical Kinetics 40 (2008) 1–18.

[35] Z. Chen, X. Qin, Y. Ju, Z. Zhao, M. Chaos, and F. L. Dryer, High temperature ignition and combustion enhancement by dimethyl ether addition to methane–air mixtures, Proceedings of the Combustion Institute 31 (2007) 1215–1222.

[36] H. Yu, E. Hu, Y. Cheng, X. Zhang, and Z. Huang, Experimental and numerical study of laminar premixed dimethyl ether/methane–air flame, Fuel 136 (2014) 37–45.

[37] P. Dai, Z. Chen, and S. Chen, Ignition of methane with hydrogen and dimethyl ether addition, Fuel 118 (2014) 1–8.

[38] T. Poinsot and S. Lele, Boundary conditions for direct simulations of compressible viscous flows, Journal of Computational Physics 101 (1992) 104–129.

[39] D. G. Goodwin, H. K. Moffat, and R. L. Speth, Cantera: An Object-oriented Software Toolkit for Chemical Kinetics, Thermodynamics, and Transport Processes, Version 2.2.1 (2016).

[40] C. K. Law, Combustion physics, Cambridge University Press, 2010.

[41] P. Habisreuther, F. C. C. Galeazzo, C. Prathap, and N. Zarzalis, Structure of laminar premixed flames of methane near the auto-ignition limit, Combustion and Flame 160 (2013) 2770–2782.

[42] R. L. Gordon, A. R. Masri, S. B. Pope, and G. M. Goldin, Transport budgets in turbulent lifted flames of methane autoigniting in a vitiated co-flow, Combustion and Flame 151 (2007) 495–511.

[43] M. B. Luong, R. Sankaran, G. H. Yu, S. H. Chung, and C. S. Yoo, On the effect of injection timing on the ignition of lean PRF/air/EGR mixtures under direct dual fuel stratification conditions, Combustion and Flame 183 (2017) 309–321.

[44] R. Sankaran and H. G. Im, Dynamic flammability limits of methane/air premixed flames with mixture composition fluctuations, Proceedings of the Combustion Institute 29 (2002) 77–84.

[45] T. Echekki and J. H. Chen, Analysis of the contribution of curvature to premixed flame propagation, Combustion and Flame 118 (1999) 308–311.

[46] H. Yamada, K. Suzaki, H. Sakanashi, N. Choi, and A. Tezaki, Kinetic measurements in homogeneous charge compression of dimethyl ether: role of intermediate formaldehyde controlling chain branching in the low-temperature oxidation mechanism, Combustion and Flame 140 (2005) 24–33.

[47] V. V. Lissianski, V. M. Zamansky, and W. C. Gardiner, Combustion chemistry modeling, in: Gas-Phase Combustion Chemistry, Springer, 2000, pp. 1–123.